

Evidence for two energy gaps and Fermi liquid behavior in the SrPt_2As_2 superconductor

Xiaofeng Xu,^{1,*} B. Chen,¹ W. H. Jiao,² Bin Chen,^{3,1} C. Q. Niu,¹ Y. K. Li,¹ J. H. Yang,¹ A. F. Bangura,⁴ Q. L. Ye,¹ C. Cao,¹ J. H. Dai,¹ Guanhao Cao,^{2,†} and N. E. Hussey⁵

¹Department of Physics, Hangzhou Normal University, Hangzhou 310036, China

²State Key Lab of Silicon Materials and Department of Physics, Zhejiang University, Hangzhou 310027, China

³Department of Physics, University of Shanghai for Science & Technology, Shanghai, China

⁴RIKEN (The Institute of Physical and Chemical Research), Wako, Saitama 351-0198, Japan

⁵H. H. Wills Physics Laboratory, University of Bristol, Tyndall Avenue, BS8 1TL, United Kingdom

(Received 27 March 2013; revised manuscript received 6 June 2013; published 17 June 2013)

We report a detailed calorimetric study on single crystals of the 5d-transition metal pnictide SrPt_2As_2 with a superconducting critical temperature $T_c \sim 5$ K. The peculiar field dependence of the electronic specific heat coefficient γ can be decomposed into two linear components. Moreover, the temperature evolution of the electronic specific heat below T_c is best described by a two-gap model. These findings suggest that two energy gaps are associated with the superconductivity. In parallel, we show that the spin-lattice relaxation time T_1 , through nuclear magnetic resonance measurement, obeys the so-called Korringa relation well. This, along with the T^2 dependence of resistivity at low temperatures, points to a Fermi liquid ground state in this material.

DOI: 10.1103/PhysRevB.87.224507

PACS number(s): 74.25.Bt, 72.15.Eb, 74.25.nj, 74.70.Xa

A central issue in the field of superconductivity is to elucidate the origin of the pairing interaction, which in turn is intimately related to the pairing symmetry and the gap structure $\Delta(k)$. Notably, nodal d -wave superconductivity with $d_{x^2-y^2}$ pairing symmetry in cuprates is generally believed to originate from the generic spin fluctuations in CuO_2 planes.¹ While in iron-based pnictides, the role played by antiferromagnetic spin fluctuations is largely dependent on the strength of the iron 3d electron correlation and remains controversial *albeit* a sign-reversing s_{\pm} gap structure and multiple energy gaps have been reported.^{2,3} In this regard, it is of fundamental importance to identify the gap structure in understanding the underlying mechanism for the superconducting pairing glue.

Recently, motivated by the discovery of high- T_c superconductivity in ThCr_2Si_2 -type pnictides AFe_2As_2 (where A represents alkaline-earth metals),⁴ a 5d-transition metal platinum-based 122 arsenide SrPt_2As_2 was found to be superconducting below $T_c \sim 5$ K.⁵⁻⁷ In contrast to other 122 Fe-based superconductors, this iron-free SrPt_2As_2 adopts a different CaBe_2Ge_2 -type structure. Its structure can be viewed as consisting of Pt_2As_2 tetrahedral layers alternating with As_2Pt_2 layers stacked along the c axis, the former layers with the Pt ion located in the center of each As tetrahedron and the latter layer the opposite.⁸ Remarkably, in analogy to Fe-based pnictides, the SrPt_2As_2 compound also shows a structural phase transition near 470 K, which is associated with charge-density-wave formation.⁷ In spite of these interesting discoveries, the nature of the low-lying quasiparticle excitations and the pairing symmetry have yet to be addressed, in particular the role of the electron-phonon interaction.

In this context, we investigate here the superconductivity of single crystals SrPt_2As_2 via detailed heat capacity measurement, a bulk probe of the low-lying quasiparticle excitations. Its calorimetric responses, including the field evolution and the temperature dependence of the quasiparticle specific heat, are overall consistent with a scenario of two s -wave superconducting gaps opening on different sections of the Fermi surface. We therefore demonstrate that SrPt_2As_2 , along with

the textbook example MgB_2 ,⁹ is another prototypical two-gap superconductor. In addition, we show from nuclear magnetic resonance (NMR) measurement that spin fluctuations play only a minor role here. The observation of the Korringa law in this material is consistent with T^2 resistivity at low temperatures, both pointing to a Fermi liquid ground state.

Single crystals of SrPt_2As_2 were synthesized by self-melting technique, following the procedure described in Ref. 7. Good single crystallinity of the as-grown samples was then confirmed by x-ray diffraction. For the transport measurements, the sample was cut into a barlike shape with the longest dimension along the basal plane. The specific heat measurement was performed on a large piece of single crystal of weight 1.3 mg using a commercial Quantum Design PPMS-9 system. The thermometer on the calorimeter puck was well calibrated prior to the measurements in various magnetic fields used in this study between 10 K down to ^3He temperature. The addenda was determined in a separate run. Finally, we also performed a ^{195}Pt NMR study to investigate the role of spin fluctuations and the Fermi liquid behavior in this material.

Figure 1 encapsulates the zero-field resistivity and the extracted upper critical field H_{c2} of SrPt_2As_2 . The temperature dependence of the resistivity is shown in part (a) of this figure and is typical of the behavior reported in the literature, i.e., metallic behavior persisting to low temperature where superconductivity eventually emerges below $T_c \sim 5$ K. The associated H_{c2} (note that the field is applied in the basal plane, $H \perp c$) was then determined from both field and temperature sweeps, as shown in Figs. 1(b) and 1(c), respectively. The 90% criterion was used to determine H_{c2} , i.e., the field (temperature) at which ρ reaches 90% of ρ_n , the resistivity of the normal state. The as-drawn H_{c2} was then depicted in Fig. 1(d) in which the data from Fang *et al.* was also reproduced for comparison.⁷ Clearly, our data overlap with those of Fang *et al.* down to the lowest temperature they studied, and persist in going up to 4 T at 0.5 K. We fit our data with the conventional one-band Werthamer-Helfand-Hohenberg (WHH) theory,¹⁰ as displayed in Fig. 1(d), by taking the initial slope near

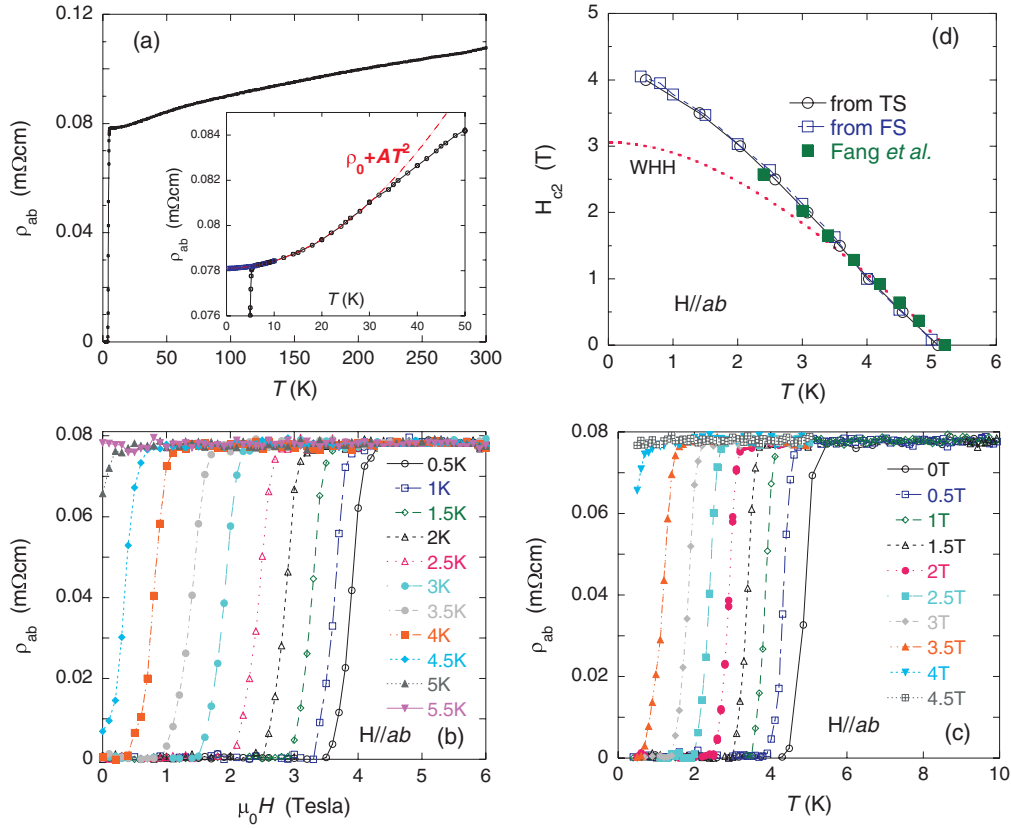


FIG. 1. (Color online) (a) Temperature dependence of the zero-field in-plane resistivity. The inset zooms in the low-temperature part with blue squares representing the data extracted from the field sweeps at fixed temperatures (see text). The red line is the fit to $\rho_0 + AT^2$. (b) and (c) Field sweep (FS) and the temperature sweep (TS), respectively, $H \perp c$, with the extracted H_{c2} presented in (d), where the data from Fang *et al.* are also plotted for comparison.⁷ The red dashed line in (d) is the WHH fit of H_{c2} .¹⁰

T_c , $(dH_{c2}^{\perp}/dT)|_{T=T_c} = 0.92$ T/K. Apparently, this one-band WHH theory cannot fit our low temperature data satisfactorily. In addition, we uncover another interesting feature of its normal state transport. As we see from Fig. 1(b), there is almost no magnetoresistance in the normal state of SrPt_2As_2 , evidenced from the flat feature of $\rho(H)$ curves above H_{c2} . This is presumably due to the strong impurity scattering deduced from the large residual resistivity. As a consequence of this, the $\rho(9$ T) data, or equivalently the intercept at $H = 0$ by linearly extrapolating the $\rho_{ab}(T, H)$ above H_{c2} ,¹¹ plotted as blue squares in the inset of Fig. 1(a), effectively represents the genuine normal state resistivity at each temperature indicated. We find that the normal state resistivity of SrPt_2As_2 is well fitted by $\rho_0 + AT^2$ up to $T \sim 32$ K, a hallmark of the Fermi liquid ground state of a metal, with $A = 3.2 \pm 0.4$ nΩ cm/K².

The failure of WHH fitting may be seen, for example, in the Fulde-Ferrell-Larkin-Ovchinnikov (so-called FFLO) state,^{12,13} the field-induced reentrant superconductivity,^{14,15} or some one-dimensional superconductors.¹⁶ All these possibilities can be readily ruled out. As well known to us, the necessary conditions for the FFLO state are twofold: clean limit superconductivity (mean-free path much larger than the coherence length) and a quenched orbital effect.^{12,13} The latter is parametrized by the so-called Maki parameter $\alpha_M = \sqrt{2}H_{\text{orb}}/H_p$. For the FFLO state to occur, the Maki

parameter should be larger than 1.8. As to SrPt_2As_2 , however, neither of these two conditions seem to be fulfilled. The large residual resistivity apparently argues again the clean limit of the system and the measured H_{c2} is obviously smaller than the Pauli paramagnetic limit H_p , indicating that orbital effect still plays a role. For the field-induced reentrant superconductivity and one-dimensional superconductors, H_{c2} at low temperatures was found to show upward curvature,^{14–16} which is not obviously seen in our system. Alternatively, the observed discrepancy from the WHH fitting in SrPt_2As_2 may be ascribed to other reasons, such as strong coupling¹⁷ or multiband superconductivity,¹⁸ though our other experimental findings (shown below) suggest that the latter is the more likely origin.

The specific heat data at different fields are given in Fig. 2(a). A clear heat capacity anomaly is observed at ~ 4.6 K in zero field. With increasing fields along the c axis (note here that the field is applied along the c axis, $H \parallel c$, which is under a different field configuration from the magnetoresistivity measurements described above), this anomaly is gradually suppressed to lower temperatures and ultimately disappears above ~ 2 T. As can be seen in the inset, the data above 2 T all collapse into a single curve (a tiny kink in 2 T curve is hardly visible), consistent with the H_{c2} extracted from the resistivity measurement under this field configuration.⁷ The plot of C/T versus T^2 allows us to determine the Sommerfeld coefficient

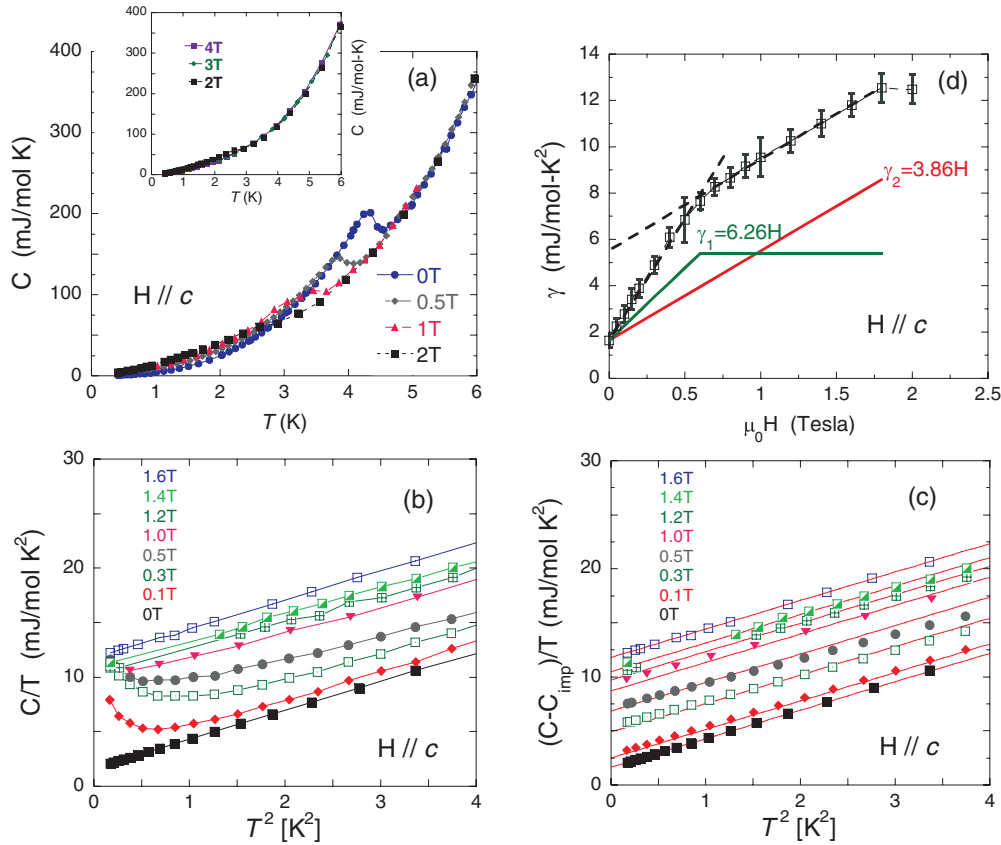


FIG. 2. (Color online) (a) Raw heat capacity data under various fields. The inset shows that the data above 2 T overlap with each other, indicative of the normal state of the sample under these fields. (b) The plot of C/T versus T^2 of the raw data. The upturns are observed in the fields between 0.1 and 1 T. Above 1 T, the upturn is not detected. (c) The plots of C/T versus T^2 after subtracting the Schottky-like upturn and the fits (the red lines) to $C/T = \gamma + \beta T^2$ that enable us to determine the γ . The slope of the fits is kept constant. The Debye temperature estimated here is ~ 160 K, slightly lower than what Fang *et al.* obtained.⁷ (d) γ coefficient as a function of field. This dependence was then decomposed into two linear components γ_1 (green) and γ_2 (red) with the slope indicated in the figure.

γ as a function of fields. Interestingly, it is noted in Fig. 2(b) that in the weak fields between 0.1 and 1 T, there are upturns in C/T at very low temperatures, the origin of which is yet unknown to us. It may be associated with the nuclear magnetic moments of ^{195}Pt or ^{75}As . However, above 1 T, no such upturns are observed. Here, we assume these low-temperature upturns are presumably due to the impurities and take the form of the Schottky anomaly, $C_{\text{imp}}/T = A(H)/T^3$. Figure 2(c) shows the C/T after the subtraction of the impurity contribution, as a function of T^2 , and the fits to $C/T = \gamma + \beta T^2$, i.e., electron and phonon terms. In this plot, the slope of each fitting line is kept constant. The resultant γ as a function of field is summarized in Fig. 2(d), with an error bar indicated for individual fields.

Figure 2(d) displays one of the key findings of this paper, namely, the resultant γ can be broken down into two linear-in-field lines up to H_{c2} . As can be seen, γ is linear in fields up to ~ 0.6 T, where it changes the slope but keeps growing linearly with fields and finally saturates at ~ 1.8 T. It is well known that in a type-II s -wave superconductor, γ increases linearly with field due to the fact that the thermal excitations mainly arise from the vortex core contribution in an s -wave superconductor and the number of the vortices grows linearly in H .¹⁹ In the clean limit of d -wave superconductors, however, $\gamma(H)$ scales

as \sqrt{H} owing to the Doppler shift of the quasiparticle spectrum near the line nodes of the gap.^{20,21} Here in SrPt_2As_2 , neither simple s -wave nor clean d -wave models explain the observed $\gamma(H)$ curve.²² Instead, reminiscent of other prototypical two-gap superconductors like MgB_2 ,⁹ $\text{Lu}_2\text{Fe}_3\text{Si}_5$,^{23,24} and Chevrel Phases,²⁵ where $\gamma(H)$ shares a wealth of similarities with the present compound, the peculiar shape of $\gamma(H)$ here can also be understood in a scheme of a two-band model. Consequently, in Fig. 2(d), we decomposed $\gamma(H)$ into two linear terms γ_1 and γ_2 , with γ_2 linear up to 1.8 T while γ_1 saturates at 0.6 T. This corresponds to $\frac{\xi_1}{\xi_2} = \sqrt{\frac{H_{c2}^{(2)}}{H_{c2}^{(1)}}} = \sqrt{3}$. Assuming the same Fermi velocities on these two bands, this immediately reveals Δ_2 approximately 1.7 times of Δ_1 . It is also noted that there is a finite γ term ~ 1.7 mJ/mol K² at zero field. We attributed this to arising from the nonsuperconducting fraction of the sample, which corresponds to 13% of the total normal carriers. By subtracting this contribution, we end up with the normal state γ term for each band equal to $\gamma_n^{(1)} = 3.7 \pm 0.4$ mJ/mol K² and $\gamma_n^{(2)} = 6.9 \pm 0.6$ mJ/mol K², respectively. Moreover, taking the total γ in the normal state, ~ 12.5 mJ/mol K², and the A coefficient of the quadratic resistivity found above, we get A/γ^2 , known as the Kadowaki-Woods ratio (KWR),²⁶ of $\sim 20 \mu\Omega \text{ cm mol}^2 \text{ K}^2/\text{J}^2$.

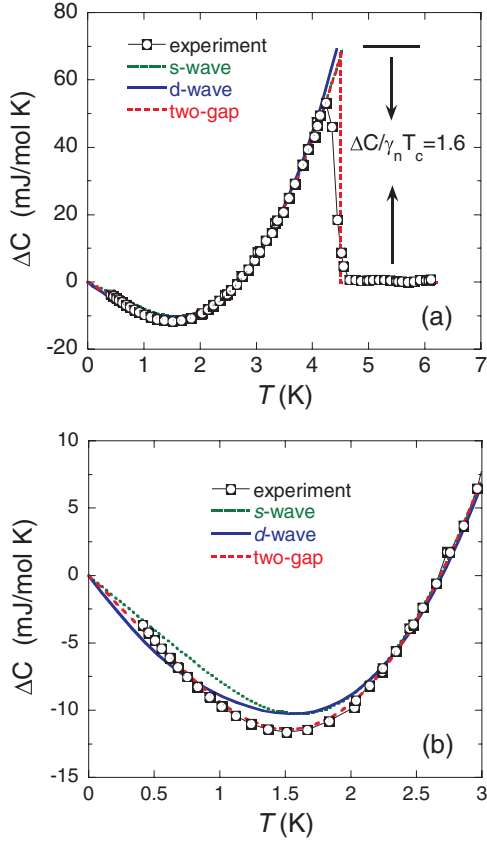


FIG. 3. (Color online) (a) Experimental data of $\Delta C = C(0\text{ T}) - C(4\text{ T})$ vs T , plotted with the fits using three different gap functions. On this large T scale, three different fits are indistinguishable. However, with the expanded view at low temperatures, panel (b), it is evident the two-gap model fits the experimental data best. The resultant $\Delta C/\gamma_n T$ for the two-gap model, as indicated in (a), is equal to 1.6, close to the weak coupling BCS value of 1.43.

Considering a fraction of the sample still being nonsuperconducting, we subtract the zero-field data with those of 4 T under which we believe the whole sample enters into the normal state, $\Delta C = C(0\text{ T}) - C(4\text{ T})$, in the same way as treated in Ref. 27. Since phonon heat capacity is field independent, ΔC removes the phonon contribution and the nonsuperconducting part, yielding $\Delta C = C_{es} - \gamma_s T$, where C_{es} is the quasiparticle contribution and γ_s here means the normal state Sommerfeld coefficient of the superconducting part. As plotted in Fig. 3(a), the heat capacity jump at T_c is best resolved in this fashion.

We analyzed our data by fitting ΔC with different gap functions, resembling what was done in Ref. 27. In BCS theory, the entropy S_{es} in the superconducting state is written as²⁷

$$S_{es} = -\frac{3\gamma_n}{k_B\pi^3} \int_0^{2\pi} \int_0^\infty [(1-f)\ln(1-f) + f\ln f] d\varepsilon d\phi, \quad (1)$$

where γ_n is the normal state γ and f stands for the quasiparticle occupation number $f = (1 + e^{E/k_B T})^{-1}$ with $E = \sqrt{\varepsilon^2 + \Delta^2(\phi)}$. $\Delta(\phi)$ is the angle dependence of the gap function. For a conventional s wave, this is angle independent, and for a standard d wave, $\Delta(\phi) = \Delta(T)\cos(2\phi)$.

TABLE I. Derived fitting parameters using Eq. (1) for three different gap functions. γ_n is in the units of mJ/mol K². The number in parentheses refers to the error bar.

	T_c (K)	α		γ_n	
s wave	4.6(0.2)	1.21(0.30)		7.97(2.52)	
d wave	4.8(0.4)	1.31(0.21)		12.23(2.05)	
Two gap	4.6(0.2)	α_1	α_2	$\gamma_n^{(1)}$	$\gamma_n^{(2)}$
		0.84(0.10)	1.27(0.21)	3.44(0.32)	6.35(0.65)

In addition, we used the well-established α model to describe the temperature dependence of the gap function, in which $\Delta(\phi, T) = \alpha \Delta_{\text{BCS}}(\phi, T)$.²⁸ Here $\Delta_{\text{BCS}}(\phi, T)$ is the weak coupling BCS gap function. Therefore, the gap is assumed to take the BCS-like form with the magnitude multiplied by a dimensionless parameter α , which gives the strength of the (electron-boson) coupling. The specific heat is thereafter calculated by $C_{es} = T(\partial S/\partial T)$. For the two-gap fitting, two sets of γ_n and α are used for each gap, respectively.

Given the small amount of sample being nonsuperconducting, we set γ_n as an adjustable parameter. Hence the free parameters in the fitting are γ_n , α , and T_c , similar to the method used in the literature.²⁷ At first sight, from Fig. 3(a), all three gap functions fit the experimental data equally well. However, the close-up view at the low temperature presented in Fig. 3(b) immediately distinguishes these three: the simple s wave does not fit the data satisfactorily nor the d -wave gap; instead, the two s -wave gap functions best capture the temperature evolution of ΔC in the whole temperature range below T_c . The corresponding fitting parameters are listed in Table I.

We now examine the two-gap fitting parameters to see their consistency with the picture we obtained thus far. First of all, the γ coefficients for each band obtained from the fitting are 3.44 and 6.35 mJ/mol K², respectively, in agreement with 3.7 ± 0.4 and 6.9 ± 0.6 mJ/mol K² extracted from Fig. 2(c). In our fitting, T_c (~ 4.6 K) is slightly higher than that defined from the zero-field anomaly in the specific heat using equal-entropy criterion (~ 4.4 K). This small discrepancy may be ascribed to any superconducting fluctuations, experimental resolution, or sample inhomogeneity, etc. In addition, the ratio of α (or equivalently Δ) values between these two gaps is 1.52, close to 1.7 obtained above by assuming the same Fermi velocity for each band. The small discrepancy may duly arise from the difference in the Fermi velocities of these two bands. Finally, this two-gap superconductivity is not conflicting with the band structure calculation where the Fermi surfaces consist of electron and hole pockets.⁸

Figure 4(a) shows the Knight shift of ¹⁹⁵Pt below 50 K, obtained from the peak resonance field as exemplified at 30 K in the inset. The T independence of the observed Knight shift indicates the nearly constant spin susceptibility, consistent with the bulk susceptibility measurement which is predominated by T -independent Pauli paramagnetism (data not shown here). The spin-lattice relaxation rate $1/T_1$ was measured at the peak position of the field-swept NMR spectrum, and determined by fitting the recovery curve to a single exponential function [$\propto \exp(-t/T_1)$] at each fixed temperature.

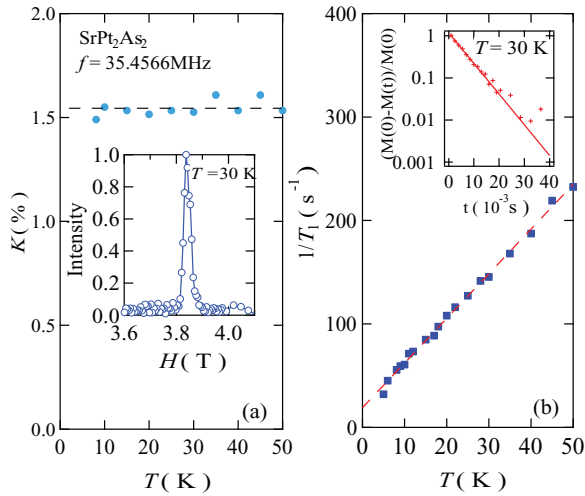


FIG. 4. (Color online) (a) Temperature dependence of ^{195}Pt Knight shift for SrPt_2As_2 . As an example, the inset shows the field-swept ^{195}Pt -NMR spectra at 30 K measured with the fixed frequency of 35.4566 MHz. (b) Temperature dependence of the ^{195}Pt nuclear spin-lattice relaxation rate $1/T_1$. The dotted line is the fit to the Korringa relation $T_1 T = \text{const}$. The inset shows the typical recovery curve measured at 30 K.

As plotted in Fig. 4(b), $1/T_1$ increases monotonically with temperature in the whole temperature range studied. The linear temperature dependence of $1/T_1$, known as the Korringa relation $T_1 T = \text{const}$, is generally believed to arise from the Fermi liquid excitations in a metal. This linear relation yields $T_1 T = 0.23 \text{ s K}$ for ^{195}Pt . Interestingly, this type of behavior had also been observed in MgB_2 by ^{25}Mg and ^{11}B NMR measurements.^{29,30} The validity of the Korringa relation in this compound, together with its T^2 resistivity at low temperatures, is indicative of a Fermi liquid ground state.

In summary, based on the experimental probes used in this study, namely, the (magneto)transport, the specific heat, as well as the NMR measurements, a coherent picture can be achieved within the framework of two-gap, s -wave, BCS-like superconductivity developed on the background of a Fermi liquid. The observed superconductivity in this material is seemingly difficult to associate with any spin fluctuations, while the role of the orbital fluctuations is not clear here. Theoretically, the frustration between the electron-hole interband interaction and the electron-electron intraband scattering can induce a nodal gap.^{31,32} However, this does not seem to be seen here. The observed two-gap energy structure, like the case of MgB_2 , seems to suggest the coupling between different bands is rather weak.⁹ Significantly, it is well known that, in $5d$ electron systems, the Coulomb interaction is relatively weak while the spin-orbit coupling could play an essential role in the electronic structures and their possible superconductivity. Yet, this role may not be always as prominent as previously thought, because it can be weakened near the Fermi surface as evidenced in another platinum-based pnictide SrPt_3P ,³³ where the superconductivity with $T_c \sim 8.4 \text{ K}$ and strong coupling to bosonic modes were observed.³⁴ Finally, the resultant KWR from our measurements is found to be $\sim 20 \mu\Omega \text{ mol}^2 \text{ K}^2/\text{J}^2$, i.e., comparable with those found for heavy fermions and other strongly correlated oxides and two orders of magnitude greater than typical values seen in transition metals. Taken at face value, this potentially indicates very strong electron-electron correlations. In this regard, it would be very interesting to explore the correlation effect in this $5d$ electron system.^{35,36}

The authors would like to acknowledge valuable discussions with Xiaofeng Jin, Y. Matsuda, T. Shibauchi, and C. M. J. Andrew, and the technical support from X. X. Yang and H. D. Wang. This work was supported by the National Natural Science Foundation of China. X.X. and C.C. acknowledge the support of Young Scientists 973 Program.

*xiaofeng.xu@hznu.edu.cn

†ghcao@zju.edu.cn

¹P. A. Lee, N. Nagaosa, and X. G. Wen, *Rev. Mod. Phys.* **78**, 17 (2006).

²P. J. Hirschfeld, M. K. Korshunov, and I. I. Mazin, *Rep. Prog. Phys.* **74**, 124508 (2011).

³J. Hu and H. Ding, *ISSI Sci. Rep.* **2**, 381 (2012).

⁴M. Rotter, M. Tegel, and D. Johrendt, *Phys. Rev. Lett.* **101**, 107006 (2008).

⁵A. Imre, A. Hellmann, G. Wenski, J. Grap, D. Johrendt, and A. Mewis, *Z. Anorg. Allg. Chem.* **633**, 2037 (2007).

⁶K. Kudo, Y. Nishikubo, and M. Nohara, *J. Phys. Soc. Jpn.* **79**, 123710 (2010).

⁷A. Fang, T. Dong, H. P. Wang, Z. G. Chen, B. Cheng, Y. G. Shi, P. Zheng, G. Xu, L. Wang, J. Q. Li, and N. L. Wang, *Phys. Rev. B* **85**, 184520 (2012).

⁸I. R. Shein and A. L. Ivanovskii, *Phys. Rev. B* **83**, 104501 (2011).

⁹F. Bouquet, Y. Wang, I. Sheikin, T. Plackowski, A. Junod, S. Lee, and S. Tajima, *Phys. Rev. Lett.* **89**, 257001 (2002).

¹⁰N. R. Werthamer, E. Helfand, and P. C. Hohenberg, *Phys. Rev.* **147**, 295 (1966).

¹¹R. A. Cooper, Y. Wang, B. Vignolle, O. J. Lipscombe, S. M. Hayden, Y. Tanabe, T. Adachi, Y. Koike, M. Nohara, H. Takagi, C. Proust, and N. E. Hussey, *Science* **323**, 603 (2009).

¹²R. Beyer, B. Bergk, S. Yasin, J. A. Schlueter, and J. Wosnitza, *Phys. Rev. Lett.* **109**, 027003 (2012).

¹³R. Lortz, Y. Wang, A. Demuer, P. H. M. Bottger, B. Bergk, G. Zwacknagl, Y. Nakazawa, and J. Wosnitza, *Phys. Rev. Lett.* **99**, 187002 (2007).

¹⁴A. G. Lebed and K. Yamaji, *Phys. Rev. Lett.* **80**, 2697 (1998).

¹⁵A. G. Lebed, *Phys. Rev. B* **59**, 721 (1999).

¹⁶Y. Fuseya, C. Bourbonnais, and K. Miyake, *Europhys. Lett.* **100**, 57008 (2012).

¹⁷J. P. Carbotte, *Rev. Mod. Phys.* **62**, 1027 (1990).

¹⁸F. Hunte, J. Jaroszynski, A. Gurevich, D. C. Larbalestier, R. Jin, A. S. Sefat, M. A. McGuire, B. C. Sales, D. K. Christen, and D. Mandrus, *Nature (London)* **453**, 903 (2008).

¹⁹N. Nakai, P. Miranovic, M. Ichioka, and K. Machida, *Phys. Rev. B* **70**, 100503 (2004).

- ²⁰Y. Matsuda, K. Izawa, and I. Vekhter, *J. Phys.: Condens. Matter* **18**, R705 (2006).
- ²¹N. E. Hussey, *Adv. Phys.* **51**, 1685 (2002).
- ²²Fits to a model of dirty d -wave superconductivity, where γ scales as $H \log(c/H)$ in weak fields,²¹ work reasonably well. However, note that this $H \log(c/H)$ scaling works for dirty d -wave superconductors only below a crossover field much lower than H_{c2} (cf. p. 1714 of Ref. 21). The reasonably good fitting of our experimental data to this model is only coincidence.
- ²³Y. Nakajima, T. Nakagawa, T. Tamegai, and H. Harima, *Phys. Rev. Lett.* **100**, 157001 (2008).
- ²⁴Y. Nakajima, H. Hidaka, T. Nakagawa, T. Tamegai, T. Nishizaki, T. Sasaki, and N. Kobayashi, *Phys. Rev. B* **85**, 174524 (2012).
- ²⁵A. P. Petrović *et al.*, *Phys. Rev. Lett.* **106**, 017003 (2011).
- ²⁶K. Kadowaki and S. B. Woods, *Solid State Commun.* **58**, 507 (1986).
- ²⁷O. J. Taylor, A. Carrington, and J. A. Schlueter, *Phys. Rev. Lett.* **99**, 057001 (2007).
- ²⁸H. Padamsee, J. E. Neighbor, and C. A. Shiffman, *J. Low Temp. Phys.* **12**, 387 (1973).
- ²⁹M. Mali, J. Roos, A. Shengelaya, H. Keller, and K. Conder, *Phys. Rev. B* **65**, 100518(R) (2002).
- ³⁰C. S. Lue, T. H. Su, B. X. Xie, S. K. Chen, J. L. MacManus-Driscoll, Y. K. Kuo, and H. D. Yang, *Phys. Rev. B* **73**, 214505 (2006).
- ³¹K. Kuroki, H. Usui, S. Onari, R. Arita, and H. Aoki, *Phys. Rev. B* **79**, 224511 (2009).
- ³²S. Kasahara, K. Hashimoto, H. Ikeda, T. Terashima, Y. Matsuda, and T. Shibauchi, *Phys. Rev. B* **85**, 060503 (2012).
- ³³H. Chen, X. Xu, C. Cao, and J. Dai, *Phys. Rev. B* **86**, 125116 (2012).
- ³⁴T. Takayama, K. Kuwano, D. Hirai, Y. Katsura, A. Yamamoto, and H. Takagi, *Phys. Rev. Lett.* **108**, 237001 (2012).
- ³⁵N. E. Hussey, *J. Phys. Soc. Jpn.* **74**, 1107 (2005).
- ³⁶A. C. Jacko *et al.*, *Nature Phys.* **5**, 422 (2009).